

Received: 2017.11.14
Accepted: 2018.03.05
Published: 2018.07.12

Expression of microRNA-99a-3p in Prostate Cancer Based on Bioinformatics Data and Meta-Analysis of a Literature Review of 965 Cases

Authors' Contribution:
Study Design A
Data Collection B
Statistical Analysis C
Data Interpretation D
Manuscript Preparation E
Literature Search F
Funds Collection G

ABCDEF 1 **Hai-biao Yan**
C 2 **Yu Zhang**
B 2 **Jie-mei Cen**
B 3 **Xiao Wang**
B 2 **Bin-liang Gan**
B 2 **Jia-cheng Huang**
F 2 **Jia-yi Li**
D 2 **Qian-hui Song**
G 1 **Sheng-hua Li**
ACEF 2 **Gang Chen**

1 Department of Urology, First Affiliated Hospital of Guangxi Medical University, Nanning, Guangxi, P.R. China
2 Department of Pathology, First Affiliated Hospital of Guangxi Medical University, Nanning, Guangxi, P.R. China
3 Department of Orthopedics, Shandong Provincial Hospital Affiliated with Shandong University, Jinan, Shandong, P.R. China

Corresponding Author: Sheng-hua Li, e-mail: 13877115066@163.com

Source of support: The study was supported by the Fund of Guangxi Zhuang Autonomous Region University, Student Future Academic Star (WLXSZX17015)

Background: microRNAs (miRNAs) have a role as biomarkers in human cancer. The aim of this study was to use bioinformatics data, and review of cases identified from the literature, to investigate the role of microRNA-99a-3p (miR-99a-3p) in prostate cancer, including the identification of its target genes and signaling pathways.

Material/Methods: Meta-analysis from a literature review included 965 cases of prostate cancer. Bioinformatics databases interrogated for miR-99a-3p in prostate cancer included The Cancer Genome Atlas (TCGA), the Gene Expression Omnibus (GEO), and ArrayExpress. Twelve computational predictive algorithms were developed to integrate miR-99a-3p target gene prediction data. Bioinformatics analysis data from Gene Ontology (GO), the Kyoto Encyclopedia of Genes and Genomes (KEGG), and protein-protein interaction (PPI) network analysis were used to investigate the possible pathways and target genes for miR-99a-3p in prostate cancer.

Results: TCGA data showed that miR-99a was down-regulated in prostate cancer when compared with normal prostate tissue. Receiver-operating characteristic (ROC) curve area under the curve (AUC) for miR-99a-3p was 0.660 (95% CI, 0.587–0.732) or a moderate level of discriminations. Pathway analysis showed that miR-99a-3p was associated with the Wnt and vascular endothelial growth factor (VEGF) signaling pathways. The *PPP3CA* and *HYOU1* genes, selected from the PPI network, were highly expressed in prostate cancer tissue compared with normal prostate tissue, and negatively correlated with the expression of miR-99a-3p.

Conclusions: In prostate cancer, miR-99a-3p expression was associated with the Wnt and VEGF signaling pathways, which might inhibit the expression of *PPP3CA* or *HYOU1*.

MeSH Keywords: **Afferent Pathways • MicroRNAs • Prostatic Neoplasms**

Abbreviations: **TCGA** – The Cancer Genome Atlas; **GEO** – Gene Expression Omnibus; **GO** – Gene Ontology; **KEGG** – Kyoto Encyclopedia of Genes and Genomes; **PPI** – protein-protein interaction; **AUC** – area under the curve; **ROC** – receiver-operating characteristic; **miRNA** – microRNA; **FP** – false positives; **TP** – true positives; **TN** – true negatives; **FN** – false negatives; **BP** – biological process; **CC** – cellular component; **MF** – molecular function; **STRING** – Search Tool for the Retrieval of Interacting Genes; **SMD** – standard mean deviation

Full-text PDF: <https://www.medscimonit.com/abstract/index/idArt/908057>

 3043

 4

 12

 55



Background

Worldwide, prostate cancer is one of the most common causes of cancer death in the male population [1,2]. In recent years, surgical prostatectomy, radiotherapy, hormone therapy, and immunotherapy have been the major methods used to treat prostate cancer, but treatment options remain limited in advanced-stage disease [3–7]. High rates of metastasis and cancer-associated mortality worsen the prognoses of prostate cancer patients, especially for patients with advanced-stage prostate cancer [8–10]. It is important to continue to study the molecular mechanisms involved in prostate cancer, which may provide novel perspectives on the diagnosis and treatment of prostate cancer patients in the future.

There is increasing published evidence that has shown that small regulatory noncoding RNAs, such as microRNAs (miRNAs) have a role as biomarkers in human cancer, and are involved in RNA silencing and the down-regulation of gene expression [11–14]. Several studies have confirmed that miRNAs play important roles in the development and progression of many types of human cancers [1,15–18]. The miRNAs may promote tumor development and progression by combining with the 3'-untranslated region (3'-UTR) of target mRNAs [19,20]. Currently, several studies have shown the expression and potential role of microRNA-99a-3p (miR-99a-3p) in cancer [21–23]. For example, miR-99a-3p has been shown to be overexpressed in colorectal cancer and may predict chemotherapy response in patients with advanced colorectal cancer [22]. Also, miR-99a-3p has been shown to be down-regulated in endometrioid endometrial carcinoma [23]. Although investigators have described the involvement of miRNAs in the biological processes of cancers, including that of miR-99a-3p, little is known about the specific mechanisms involved in the interaction between miR-99a-3p and prostate cancer [24].

The aim of this study was to explore the role and mechanism of miR-99a-3p in prostate cancer based on bioinformatics analysis and using a meta-analysis of patient data from a literature review. This study extracted original data provided by The Cancer Genome Atlas (TCGA) database, and twelve miRNA prediction algorithms were utilized to predict the target genes of miR-99a-3p. Gene expression microarrays for prostate cancer were downloaded from the Gene Expression Omnibus (GEO) to select the genes that were differentially expressed in prostate cancer. Further supporting bioinformatics analysis was included from Gene Ontology (GO), the Kyoto Encyclopedia of Genes and Genomes (KEGG), and protein-protein interaction (PPI) network analysis was applied to investigate the possible mechanism of miR-99a-3p in prostate cancer.

Material and Methods

Validation the expression of microRNA-99a-3p (miR-99a-3p) based on The Cancer Genome Atlas (TCGA), Gene Expression Omnibus (GEO), and ArrayExpress

The Cancer Genome Atlas (TCGA) (<http://cancergenome.nih.gov/>) is a database of expression profiles for at least 30 kinds of cancers, including prostate cancer [25–27]. TCGA can be used to explore clinicopathological parameters associated with patients with cancer, which were used in this study [28,29]. In the current study, the RNA sequencing (RNA-Seq) data for prostate cancer patients, which were taken from the Illumina MiSeq RNA-Seq platform, contained 498 prostate cancer cases and 52 normal prostate cases, up to 1st November 2017. The expression data for microRNA-99a-3p (miR-99a-3p) were shown in reads per million (RPM), and miR-99a-3p expression levels were normalized via the 'R' language package DESeq.

The relationship between miR-99a-3p and clinicopathological parameters in prostate cancer cases was further analyzed based on the expression data in TCGA database using a Student's t-test. The receiver-operating characteristic (ROC) curve was utilized to assess the value of miR-99a-3p levels in discriminating between prostate cancer patients and normal controls. The chip datasets from the Gene Expression Omnibus (GEO) were also searched <http://www.ncbi.nlm.nih.gov/geo/>, and the public database of microarray gene expression, ArrayExpress was used (<http://www.ebi.ac.uk/arrayexpress/>).

For database searches, the following keywords were used: prostate OR prostatic gland OR prostat* AND cancer OR carcinoma OR tumor OR neoplas* OR malignan OR adenocarcinoma AND miR OR miRNA OR microRNA OR miR OR miRNA OR microRNA. The expression data for miR-99a-3p were extracted from GEO and ArrayExpress databases.

A literature review of miR-99a-3p and prostate cancer

The prostate cancer-related miR-99a-3p microarray data in GEO and ArrayExpress and the RNA-seq data in TCGA were all downloaded. Also, this study included a literature search for for publications related to miR-99a-3p in prostate cancer in twelve online databases: PubMed, Google Scholar, Web of Science, EMBASE, Ovid, Wiley Online Library, LILACS, Science Direct, Cochrane Central Register of Controlled Trials, Chinese CNKI, Wan Fang, Chong Qing VIP, and on the China Biology Medicine disc. The retrieval date was October 30, 2017. The retrieval was performed and checked by two people (Bin-liang Gan and Jie-mei Cen). A group discussion was organized if there were any disagreements. The number of false positives (FP), true positives (TP), true negatives (TN) and false negatives (FN) were extracted.

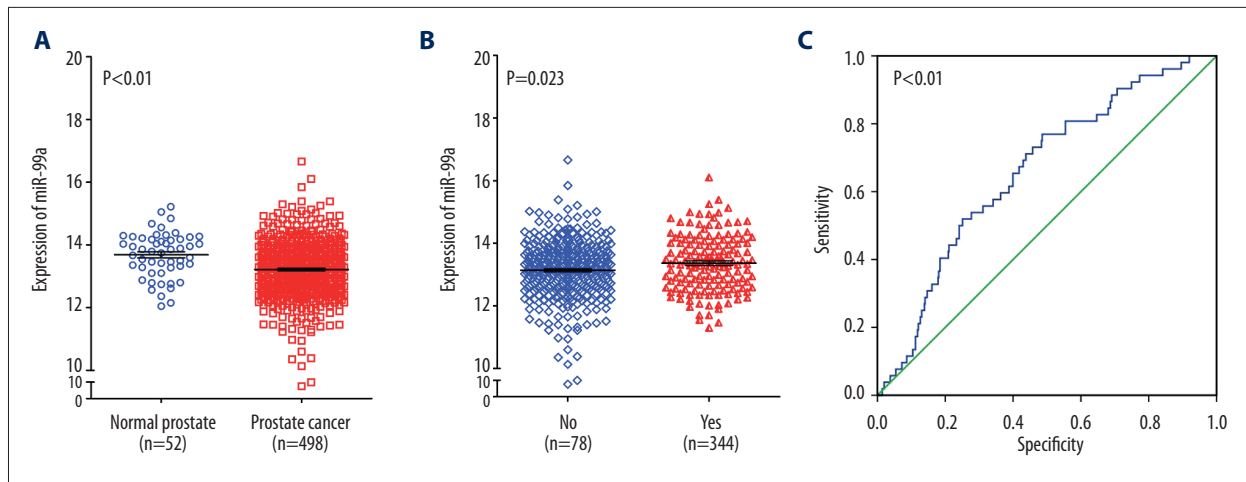


Figure 1. Clinical significance of microRNA-99a-3p (miR-99a-3p) in prostate cancer based on The Cancer Genome Atlas (TCGA) database. **(A)** Differential expression of microRNA-99a-3p (miR-99a-3p) between prostate cancer tissue and non-cancerous prostate tissue. **(B)** Differential expression of miR-99a-3p in cases with lymph node metastasis compared with those without lymph node metastasis. **(C)** The receiver-operating characteristic (ROC) curve for miR-99a-3p in prostate cancer.

Table 1. Differential expression of miR-99a and clinicopathological parameters in prostate cancer based on TCGA.

Clinicopathological features	N	miR-99a expression			
		Mean ±SD	T	P value	
Tissues	Normal prostate	52	13.685±0.722	-4.304	<0.001
	Prostate cancer	498	13.216±0.955		
Age	<60	201	13.215±0.976	0.103	0.917
	≥60	203	13.205±0.938		
Race	White	146	13.275±1.003	F=0.276	0.759
	Black	7	13.120±0.792		
	Asian	2	12.826±0.649		
Stage	I+II	187	13.265±1.016	0.153	0.347
	III+IV	300	13.182±0.918		
T (tumor)	T1+T2	348	13.219±0.904	0.190	0.349
	T3+T4	55	13.091±1.183		
N (node)	Yes	78	13.415±0.953	-2.277	0.023
	No	344	13.14±0.965		
M (metastasis)	Yes	3	12.936±1.278	0.506	0.613
	No	454	13.220±0.968		

The potential target genes of miR-99a-3p

In the present study, twelve online target prediction algorithms were selected to predict the target genes of miR-99a-3p. These twelve algorithms were used were miRWalk (<http://zmf.umm.uni-heidelberg.de/>), miRmap (<http://mirmap.ezlab.org/>), miRecords (<http://c1.accurascience.com/miRecords/>), DIANA-mT

(<http://diana.imis.athena-innovation.gr/>), miRanda (<http://www.microrna.org/>), miRDB (<http://www.mirdb.org/>), RNAhybrid (<http://bibiserv2.cebitec.uni-bielefeld.de/>), PICTAR4 (http://pictar.mdc-berlin.de/cgi-bin/PicTar_vertebrate.cgi), PICTAR5 (http://pictar.mdc-berlin.de/cgi-bin/new_PicTar_vertebrate.cgi), PITA (<http://genie.weizmann.ac.il/>), RNA22 (<http://cbcsrv.watson.ibm.com/rna22.html>), and TargetScan (<http://www>

Table 2. Characteristics of microarray datasets included in the study.

First author (publication year)	Country	Data source	Test method/ Platform	Cancer group	Normal controls	Mean1 ±SD1	Mean0 ±SD0
Taylor B. et al. (2010)	USA	GEO: GSE21036	Agilent GPL8227	113	28	3.778±0.648	4.518±0.33
Wach S. et al. (2010)	Germany	GEO: GSE23022	Affymetrix GPL8786	20	20	0.921±0.177	0.909±0.228
Mattila H. et al. (2010)	Finland	GEO: GSE24201	Agilent GPL7731	14	15	15.684±5.269	16.757±8.92
Keller A. et al. (2011)	Germany	GEO: GSE31568	Febit GPL9040	23	70	49.266±49.74	42.421±34.322
Zhong W. et al. (2012)	China	GEO: GSE34932	Agilent GPL11487	9	7	1.773±0.766	1.406±0.293
Lin P.C. et al. (2012)	USA	GEO: GSE36802	Affymetrix GPL8786	21	21	6.197±1.993	6.788±0.952
Jalava S.E. et al. (2012)	Finland	ArrayExpress: E-MTAB-408	Agilent A-MEXP-1663	28	26	3.138±0.792	1.811±1.371
TCGA (2017)	USA	TCGA	NR	498	52	13.216±0.955	13.685±0.722

Mean1 ±SD1 – prostate cancer tissues; Mean0 ±SD0 – non-tumor tissues.

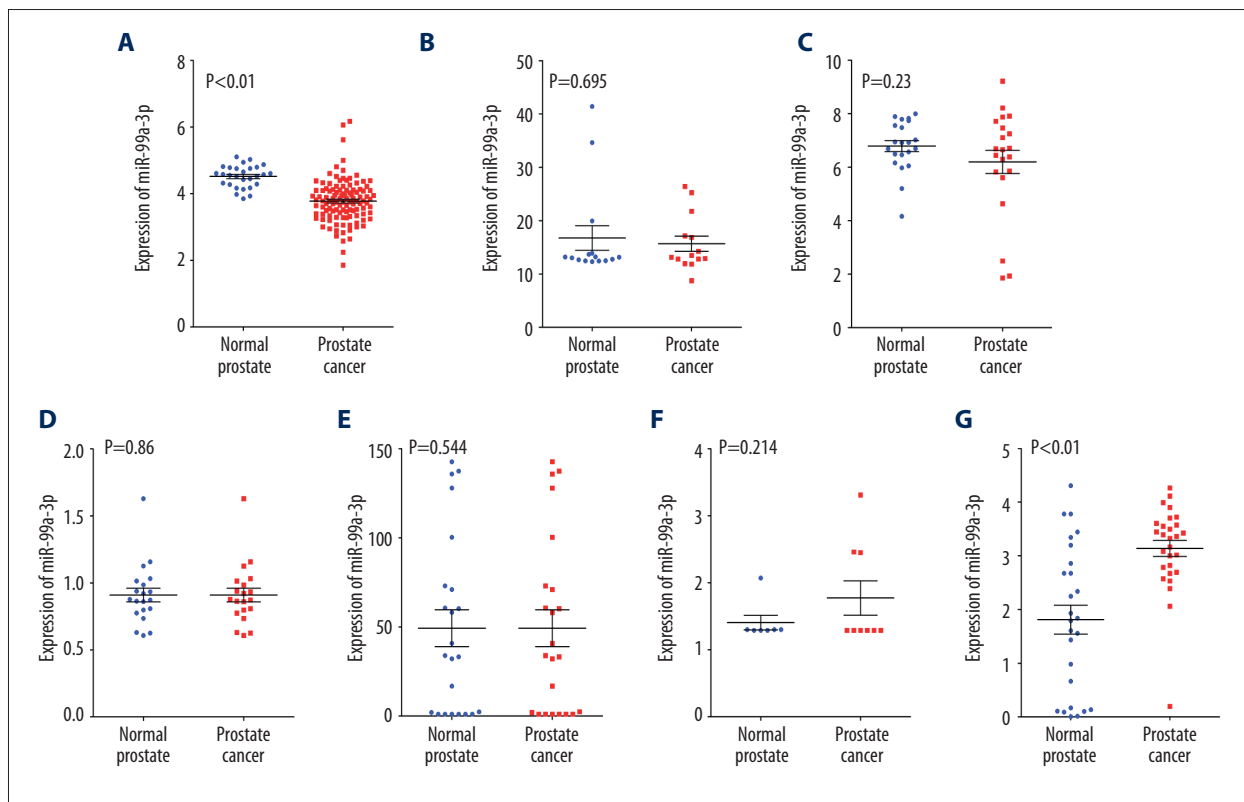


Figure 2. Differential expression of microRNA-99a-3p (miR-99a-3p) in prostate cancer based on the Gene Expression Omnibus (GEO) and ArrayExpress datasets. (A) GSE21036. (B) GSE24201. (C) GSE36802. (D) GSE23022. (E) GSE31568. (F) GSE34932. (G) E-MTAB-408.

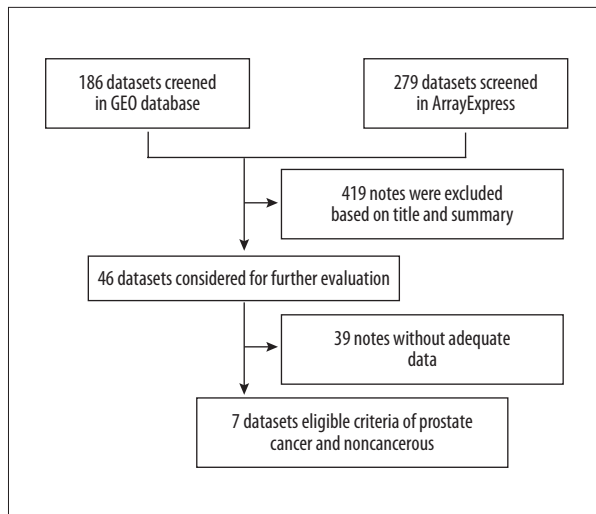


Figure 3. The procedures involved in the meta-analysis of the literature review.

targetscan.org/). A Venn diagram tool (<http://bioinformatics.psb.ugent.be/webtools/Venn/>) was chosen for the identification of candidate genes. Genes that were concurrently predicted by more than two target prediction algorithms were selected for further analysis.

Also, the gene expression microarrays for prostate cancer were downloaded from GEO using the following keywords: miR-99a-3p OR miRNA-99a-3p OR microRNA-99a-3p AND prostate OR prostatic gland OR prostat* AND cancer OR carcinoma OR tumor OR neoplas* OR malignan OR adenocarcinoma. Then, the genes that were differentially expressed in prostate cancer were selected.

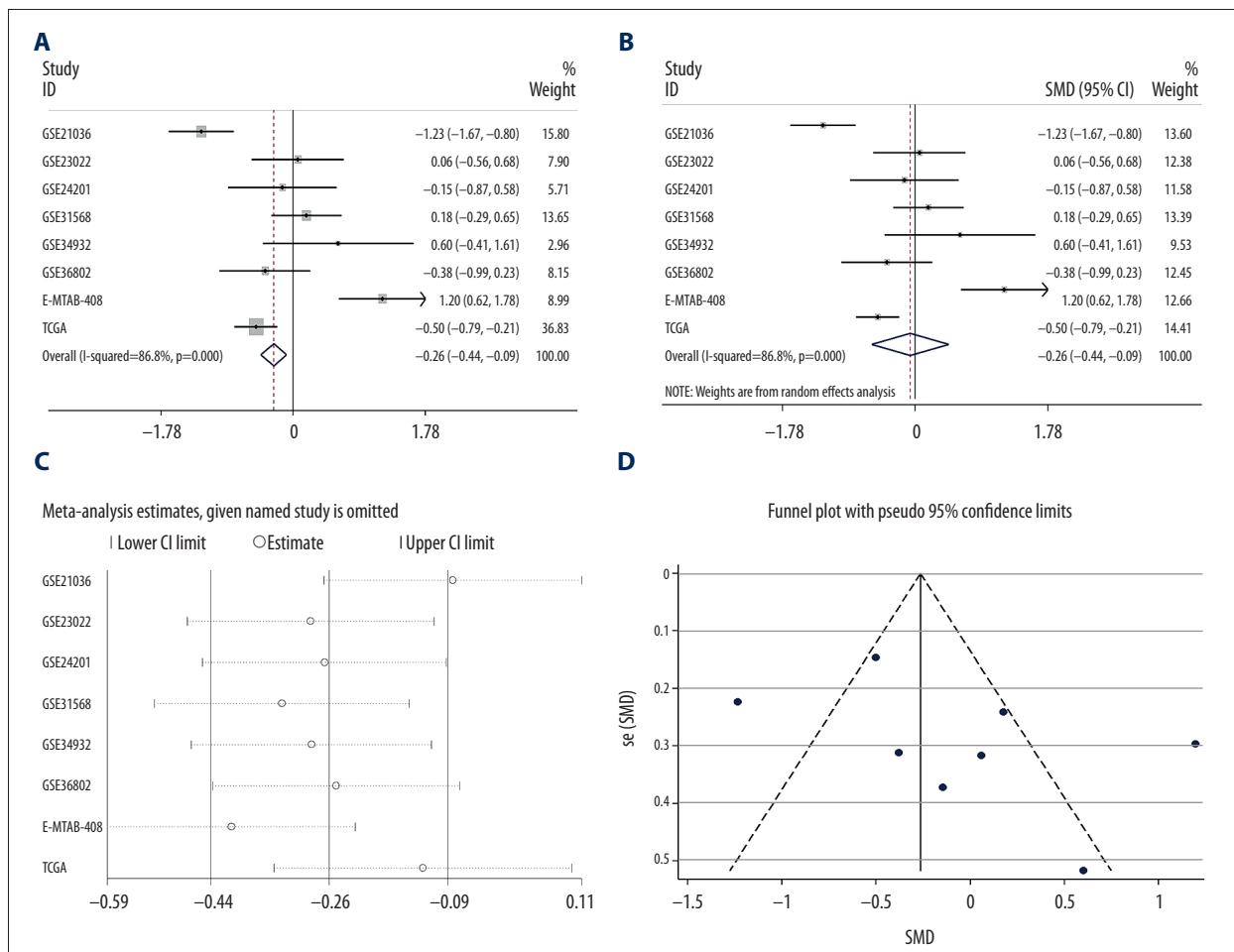


Figure 4. The expression conditions of microRNA-99a-3p (miR-99a-3p) in prostate cancer tissue compared with normal prostate tissue. (A) Forest plot of the datasets evaluating microRNA-99a-3p (miR-99a-3p) expression in prostate cancer patients compared with normal control groups (fix-effects model). (B) Forest plot of datasets evaluating miR-99a-3p expression between prostate cancer and normal control groups (random-effects model). (C) Sensitivity analysis to exclude the main studies one at a time. (D) Funnel plot of datasets, indicating that no publication bias was found in the analysis.

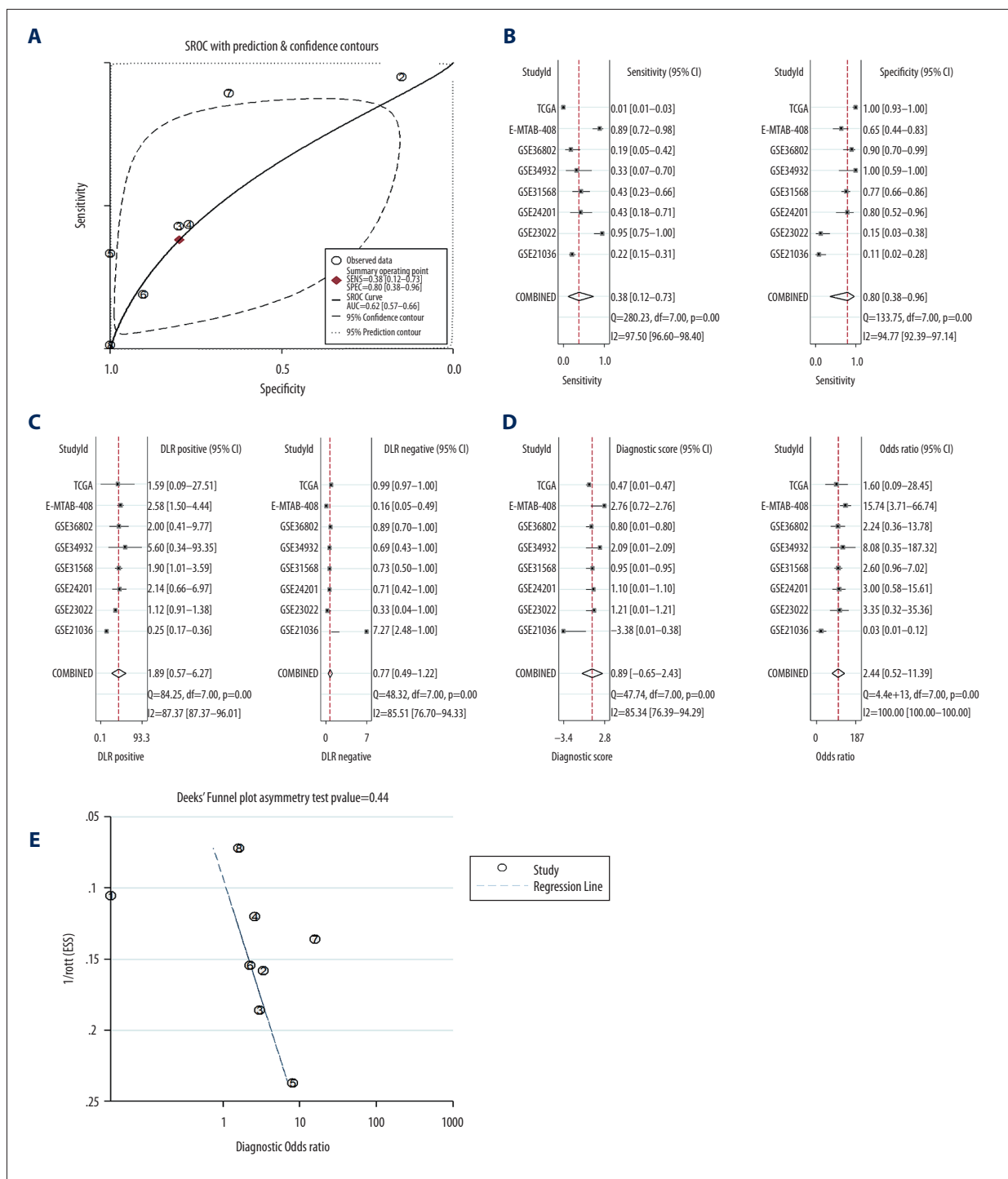


Figure 5. The meta-analysis of the literature review of published studies on microRNA-99a-3p (miR-99a-3p) and prostate cancer included 965 cases of prostate cancer. **(A)** The summary receiver-operating characteristic (SROC) curve, which represents the performance of the association of miR-99a-3p with prostate cancer, based on data from a meta-analysis. **(B)** The pooled sensitivity and specificity of the included studies. **(C)** The pooled positive diagnostic likelihood ratio (DLR) and negative DLR values of the included studies. The diagnostic DLR is the ratio of the likelihood of the observed test result in patients with prostate cancer vs. a population without prostate cancer. **(D)** The pooled diagnostic score and diagnostic odds ratio (OR) of the included studies. **(E)** The publication bias: 1/root (ESS) refers to the inverse root of the effective sample size. Each circle represents an included study.

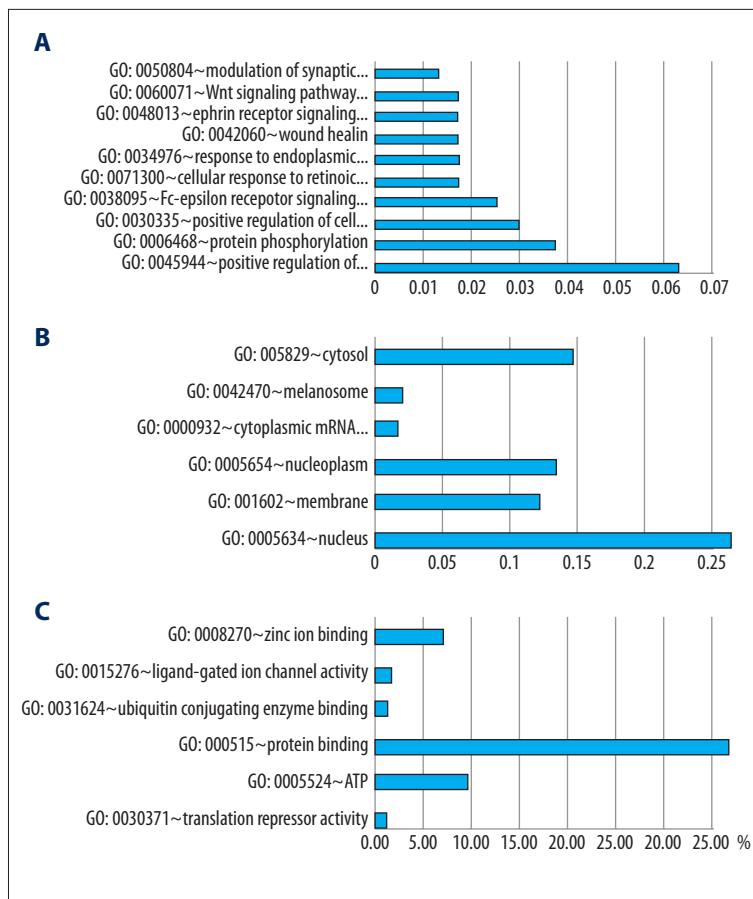


Figure 6. Distribution of Gene Ontology (GO) terms for the target genes of microRNA-99a-3p (miR-99a-3p) in prostate cancer. **(A)** Biological process (BP). **(B)** Cellular component (CC). **(C)** Molecular function (MF).

The potential functions and pathways associated with miR-99a-3p

To further explore the potential functions and pathways associated with miR-99a-3p, bioinformatics analysis, including Gene Ontology (GO), the Kyoto Encyclopedia of Genes and Genomes (KEGG), and protein-protein interaction (PPI) network analysis, were applied to study the underlying functions, networks, and pathways of the genes [30–32]. The DAVID Bioinformatics Tool (<https://david.ncifcrf.gov/>, Version 6.7) was utilized to perform the GO and KEGG analysis [33–35]. Biological process (BP), cellular component (CC) and molecular function (MF) data were exported from GO. Cytoscape (Version 3.0) (<http://cytoscape.org>) was used to create the functional network between miR-99a-3p and the potential genes.

Construction of the protein-protein interaction (PPI) network

The interaction pairs of the potential genes were surveyed by using the Search Tool for the Retrieval of Interacting Genes (STRING) Version 9.0 (<http://string-db.org>) [34,36,37]. A STRING database has been constructed to provide a global perspective for as many species as possible, including humans. The known and predicted

relationships were integrated and scored, and a combined score of >0.4 was recognized in the construction of the PPI network.

Identification of miR-99a-transcription factors (TFs)

The CircuitsDB (<http://biocluster.di.unito.it/circuits>) database is a web-server used to research miRNA transcription factor (TF) regulatory circuits in humans and mice [38]. The TFs were extracted from the CircuitsDB database, and a regulatory network was constructed between miR-99a-3p and these TFs using Cytoscape software (Version 3.0).

Statistical analysis

Statistical analysis was performed using SPSS version 22.0 (SPSS, IBM, Chicago, IL, USA). A student's t-test was carried to compare the expression of miR-99a-3p in prostate cancer and normal prostate tissue. A receiver-operating characteristic (ROC) curve was created to differentiate prostate cancer from normal prostate tissues via miR-99a-3p expression. Spearman's rank correlation coefficient was used to determine the relationship between miR-99a-3p and potentially associated genes. $P < 0.05$ (two-sided) was considered to indicate statistical significance.

Table 3. Top-six enrichment GO terms (BP, CC, and MF) of the target genes of miR-99a-3p.

ID	Term	Ontology	Count	Fold enrichment	P
GO: 0045944	Positive regulation of transcription from RNA polymerase II promoter	BP	15	1.82098163	0.034475
GO: 0006468	Protein phosphorylation	BP	9	2.350503919	0.037316
GO: 0030335	Positive regulation of cell migration	BP	7	4.530681468	0.004461
GO: 0038095	Fc-epsilon receptor signaling pathway	BP	6	4.014343772	0.016754
GO: 0071300	Cellular response to retinoic acid	BP	4	6.80526849	0.020687
GO: 0034976	Response to endoplasmic reticulum stress	BP	4	6.351583924	0.024768
GO: 0005634	Nucleus	CC	63	1.493129414	0.000222
GO: 0016020	Membrane	CC	29	1.691728553	0.005267
GO: 0005654	Nucleoplasm	CC	32	1.475149749	0.021198
GO: 0000932	Cytoplasmic mRNA processing body	CC	4	6.581437342	0.022627
GO: 0042470	Melanosome	CC	4	5.082694185	0.043657
GO: 0005829	Cytosol	CC	35	1.355001806	0.046229
GO: 0030371	Translation repressor activity	MF	3	31.75109718	0.003779
GO: 0005524	ATP binding	MF	23	1.791087533	0.008073
GO: 0005515	Protein binding	MF	88	1.166194728	0.02601
GO: 0031624	Ubiquitin conjugating enzyme binding	MF	3	11.26651835	0.02859
GO: 0015276	Ligand-gated ion channel activity	MF	3	9.701724138	0.037683
GO: 0008270	Zinc ion binding	MF	17	1.693029704	0.041044

Results

The expression of microRNA-99a-3p (miR-99a-3p) based on The Cancer Genome Atlas (TCGA), Gene Expression Omnibus (GEO), and ArrayExpress

The original data from The Cancer Genome Atlas (TCGA) was further investigated and showed that miR-99a-3p was significantly down-regulated in prostate cancer when compared with non-cancerous prostate tissues ($P < 0.001$) (Figure 1A). The relationship between miR-99a-3p and the clinicopathological parameters of prostate cancer showed that high expression levels of miR-99a-3p were positively related to lymph node metastasis ($P = 0.023$) (Figure 1B; Table 1). Also, the receiver-operating characteristic (ROC) curve showed that the area under the curve (AUC) for miR-99a was 0.660 (95% CI 0.587–0.732) ($P < 0.001$) for prostate cancer patients, which reflected the moderate level of the ability of miR-99a-3p to discriminate between prostate cancer patients and normal controls (Figure 1C). The correlations between the expression of miR-99a-3p and other clinical parameters in prostate cancer were explored, but no positive associations were identified from the TCGA data.

Also, seven clip datasets (GSE21036, GSE23022, GSE24201, GSE31568, GSE34932, GSE36802, and E-MTAB-408) were chosen based on GEO and ArrayExpress. The detailed characteristics of the microarray datasets included in the study are shown in Table 2. A Student's t-test was applied to compare miR-99a-3p expression in prostate cancer with normal prostate tissues. The down-regulated expression of miR-99a-3p in prostate cancer was found in GSE21036, GSE24201, and GSE36802, whereas GSE23022, GSE31568, GSE34932, and E-MTAB-408 showed upregulation of expression of miR-99a-3p in prostate cancer (Figure 2A–2G).

Analysis from the literature review of the association between miR-99a-3p and prostate cancer: The identification of 965 cases

The literature review identified 965 cases from three centers (six datasets from GEO, one dataset from ArrayExpress, and the original data from TCGA). The procedure involved in the analysis is shown in Figure 3. For miR-99a-3p expression in the prostate cancer group, compared with the normal group, a fixed-effect model was first used to calculate the standard

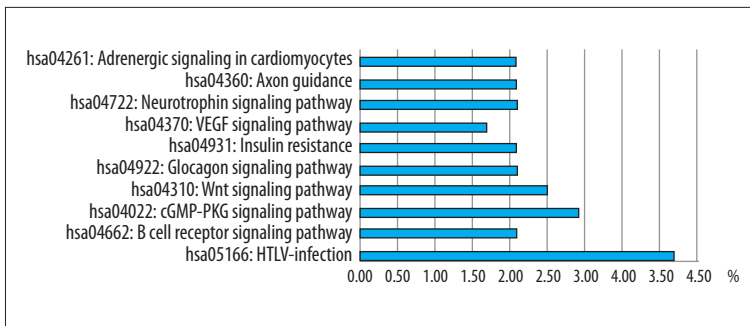


Figure 7. Distribution of the Kyoto Encyclopedia of Genes and Genomes (KEGG) terms for the target genes of microRNA-99a-3p (miR-99a-3p) in prostate cancer.

Table 4. Top-ten KEGG pathway enrichment analysis of the target genes of miR-99a-3p.

KEGG ID	KEGG term	Count	Fold Enrichment	P
hsa05166	HTLV-I infection	10	4.152644231	0.000528
hsa04662	B cell receptor signaling pathway	5	7.703455964	0.003688
hsa04022	cGMP-PKG signaling pathway	7	4.482854495	0.004163
hsa04310	Wnt signaling pathway	6	4.622073579	0.00877
hsa04922	Glucagon signaling pathway	5	5.369075369	0.013068
hsa04931	Insulin resistance	5	4.921652422	0.017494
hsa04370	VEGF signaling pathway	4	6.970996217	0.018625
hsa04722	Neurotrophin signaling pathway	5	4.429487179	0.024709
hsa04360	Axon guidance	5	4.185342217	0.029641
hsa04261	Adrenergic signaling in cardiomyocytes	5	3.640674394	0.045801

mean deviation (SMD). The combined SMD reached -0.26 ($-0.44, -0.09$), with high heterogeneity ($I^2=86.8\%$) ($P<0.05$), indicating the down-regulation of expression of miR-99a-3p in prostate cancer cases (Figure 4A).

A random-effect model was used, and the combined SMD reached -0.06 ($-0.58, 0.45$), with heterogeneity of $>50\%$ (Figure 4B). To investigate whether a certain study had contributed to this heterogeneity, a sensitivity analysis was applied, and this sensitivity analysis showed that the pooled SMD was stable (Figure 4C). Also, no significant publication bias was found (Figure 4D).

The diagnostic analysis demonstrated that the area under the curve (AUC) of the summary receiver-operating characteristic (SROC) curve was 0.62 ($0.57-0.66$) (Figure 5A), with a sensitivity and specificity of 0.38 (95% CI, $0.12-0.73$) and 0.80 (95% CI, $0.38-0.96$), respectively (Figure 5B). Also, the results confirmed the AUC (0.660) of the original data from TCGA, which indicated the moderate value of miR-99a-3p in predicting prostate cancer. The negative and positive diagnostic likelihood ratio (DLR) values were 0.77 ($0.49-1.22$) and 1.89 ($0.57-6.27$), respectively (Figure 5C). A DLR value of 1.89 suggested that

patients with prostate cancer had an approximately 1.89-fold greater chance of being miR-99a-3p assay-positive. The diagnostic score and odds ratio (OR) were 0.89 ($-0.65-2.43$) and 2.44 ($0.52-11.39$), respectively (Figure 5D). No significant publication bias was found ($P=0.44$) (Figure 5E).

Gene Ontology (GO) and the Kyoto Encyclopedia of Genes and Genomes (KEGG) pathway analysis

Based on the twelve target prediction algorithms, 1,062 genes were predicted by more than two prediction algorithms. Furthermore, only one gene dataset (GSE85614) was found to relate to miR-99a-3p in prostate cancer. Genes found to be upregulated (≥ 2 fold change) in GSE85614 were selected. A total of 5,270 differentially expressed genes were selected. Also, 156 genes were found to overlap in both prediction algorithms (1,062) and the GEO database (5,270). These 156 genes were used for the GO and pathway analysis. The GO analysis showed that the strongly enriched terms were protein phosphorylation, translation repressor activity, and protein binding (Figure 6; Table 3). The KEGG pathway analysis showed that miR-99a-3p was associated with different pathways, the Wnt and vascular endothelial growth factor (VEGF) signaling

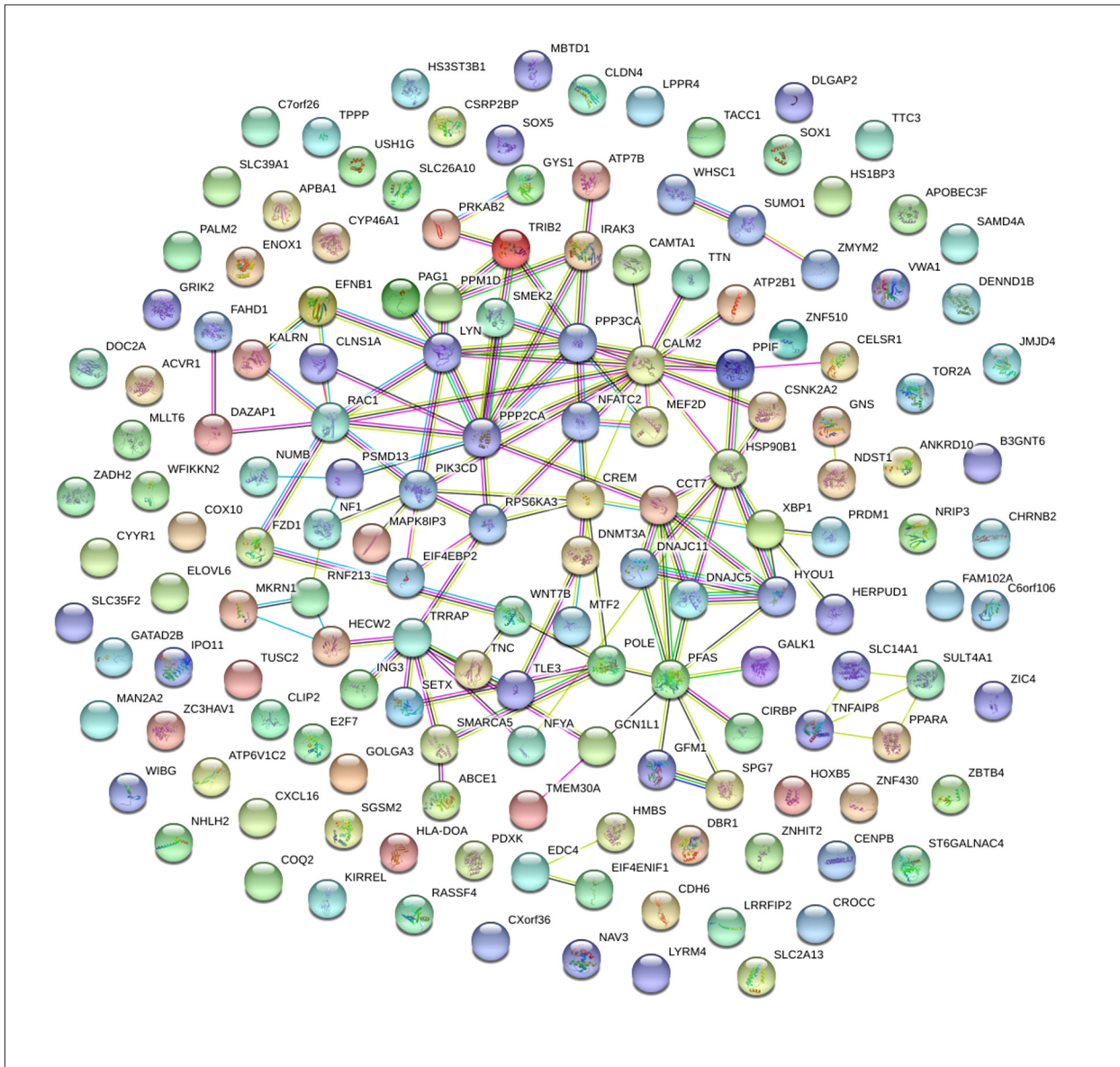


Figure 9. The protein-protein interaction (PPI) network of the target genes, created using STRING online.

Figure 11A–11D, immunostaining for PPP3CA and HYOU1 protein expression were both positive in prostate cancer tissues.

Based on the results described above, it might be possible to hypothesize that miR-99a-3p may influence the expression of the *PPP3CA* or *HYOU1* genes that encode proteins involved in prostate cancer. Figure 12 shows the regulatory network of miR-99a-3p and transcription factors, constructed using Cytoscape, an open source bioinformatics software platform to visualize molecular networks and their integrating and interaction with gene expression profiles (www.cytoscape.org).

Discussion

The initial aim of this study was to investigate the expression levels of microRNA-99a-3p (miR-99a-3p) in prostate cancer based on The Cancer Genome Atlas (TCGA), and the results showed that miR-99a-3p was down-regulated in prostate cancer compared with normal prostate tissue. The receiver operating characteristic (ROC) curve showed that miR-99a-3p might have a moderate ability to discriminate between prostate cancer patients and normal controls.

The present study was the first include a meta-analysis evaluating the expression and diagnostic value of miR-99a-3p in prostate cancer. As a result, the standard mean deviation (SMD) was

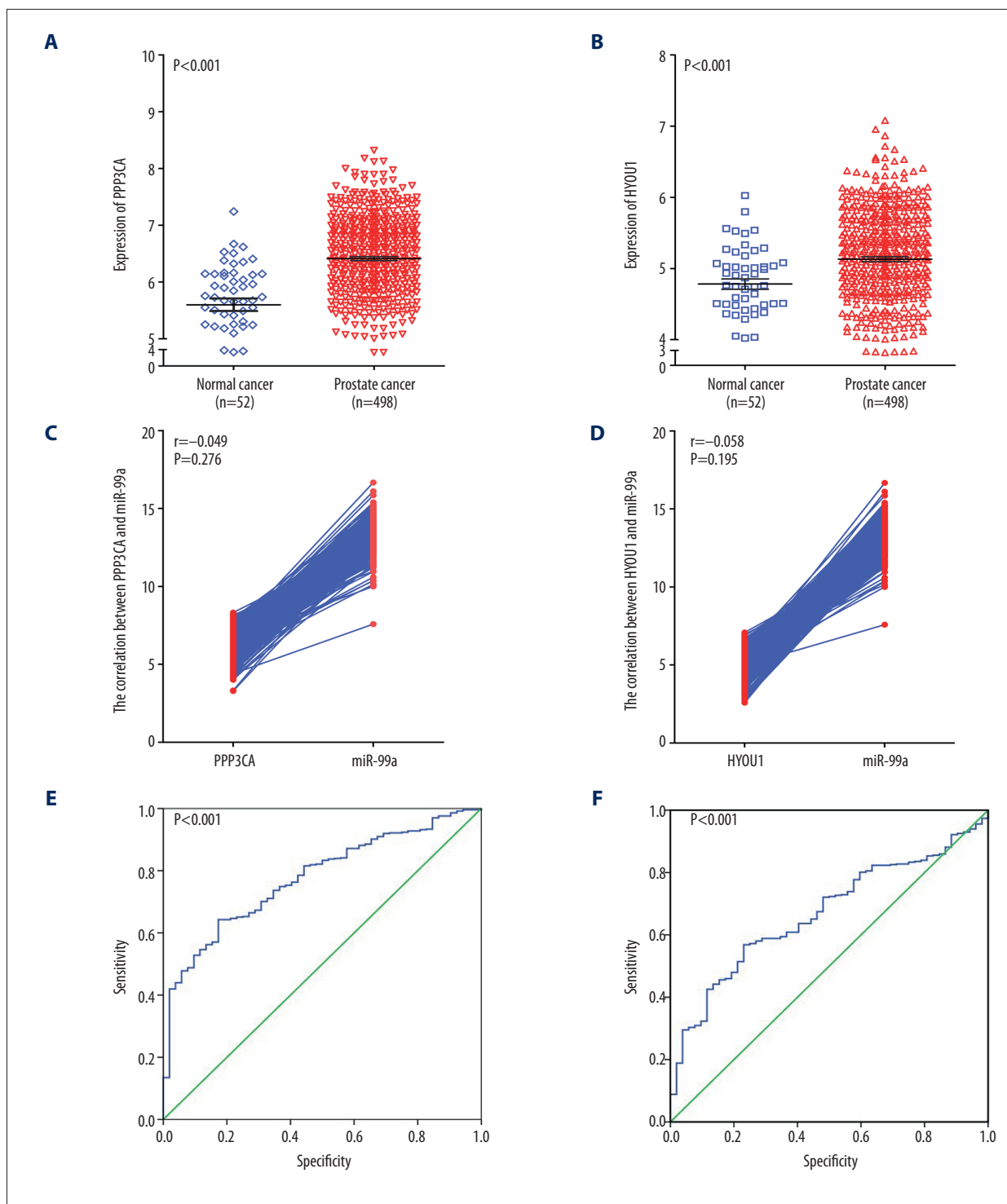


Figure 10. Clinical significance of the expression of the *PPP3CA* and *HYOU1* genes in prostate cancer, based on The Cancer Genome Atlas (TCGA) database. **(A)** The differential expression of *PPP3CA* in tissue containing prostate cancer compared with normal, non-cancerous prostate tissue. **(B)** The differential expression of *HYOU1* in tissue containing prostate cancer compared with normal, non-cancerous prostate tissue. **(C)** The negative correlation between *PPP3CA* and miR-99a-3p. **(D)** The negative correlation between *HYOU1* and miR-99a-3p. **(E)** The receiver-operating characteristic (ROC) curve for *PPP3CA* in prostate cancer. **(F)** The ROC curve for *HYOU1* in prostate cancer.

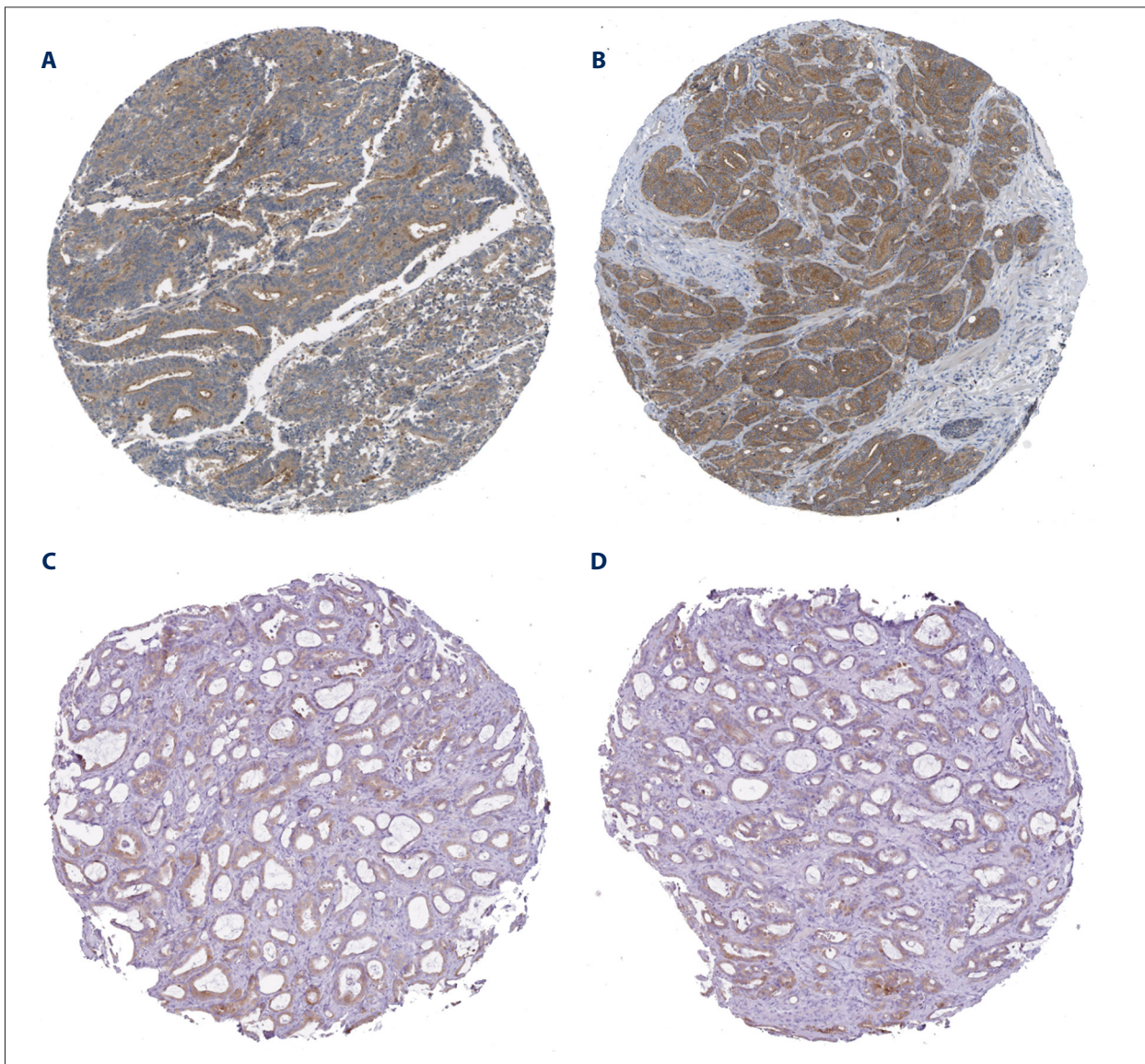


Figure 11. The immunohistochemical staining for protein phosphatase 3 catalytic subunit alpha (PPP3CA) and the hypoxia upregulated protein 1 (HYOU1) protein in prostate cancer tissues. (A, B) Prostate cancer tissues show positive immunostaining of cancer cells with antibody HPA012778 to protein phosphatase 3 catalytic subunit alpha (PPP3CA). (C, D) Prostate cancer tissues show positive immunostaining of cancer cells with antibody HPA049296 to the hypoxia upregulated protein 1 (HYOU1) protein.

-0.26 (-0.44, -0.09) and this meta-analysis verified the down-regulated expression of miR-99a-3p in prostate cancer. In the diagnostic meta-analysis, 965 cases from the Gene Expression Omnibus (GEO), TCGA, and ArrayExpress were included, and the results were utilized to assess the ability of miR-99a-3p to detect prostate cancer. However, this meta-analysis had several limitations. A high level of heterogeneity was unavoidable, partly because blinding was present in only three included databases (GEO, ArrayExpress, and TCGA). Also, the different expression trends for miR-99a-3p in GEO and ArrayExpress may also have contributed to the high heterogeneity.

To further explore the potential functions and pathways associated with miR-99a-3p, bioinformatics analysis was applied to investigate the underlying functions, pathways, and networks of the genes. The Gene Ontology (GO) terms of protein phosphorylation, translation repressor activity, and protein binding were found to be highly enriched. Also, miR-99a-3p might be associated with the Wnt and vascular endothelial growth factor (VEGF) signaling pathways.

Protein-protein interaction (PPI) network analysis was used to investigate the most likely target genes for miR-99a-3p in

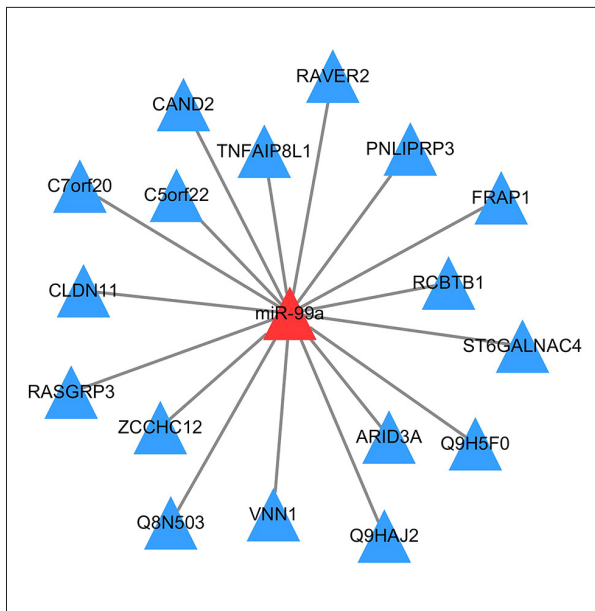


Figure 12. The regulatory network of microRNA-99a-3p (miR-99a-3p) and transcription factors, constructed using Cytoscape. Cytoscape is an open source bioinformatics software platform to visualize molecular networks and their integrating and interaction with gene expression profiles (www.cytoscape.org).

prostate cancer and *PPP2CA*, *LYN*, *TRRAP*, *PPP3CA*, *PIK3CD*, and *HYOU1* were selected. Three protein phosphatase 3 catalytic subunit alpha (*PPP3CA*) gene and the hypoxia upregulated protein 1 (*HYOU1*) gene were more highly expressed in prostate cancer tissue when compared with normal prostate tissue, and negative correlations were found between miR-99a-3p and both *PPP3CA* and *HYOU1*. Therefore, it might be possible to propose that miR-99a-3p has a role in prostate cancer by influencing *PPP3CA* or *HYOU1* gene expression and by contributing to pathways including the Wnt and VEGF signaling pathways. However, further functional studies are required to verify these preliminary findings.

Several previously published studies have confirmed the significant role of miR-99a in prostate cancer. For example, Sun et al. [19] found that miR-99 family members, including miR-99a, -99b, and -100, were all down-regulated in prostate cancer, which was consistent with the results of the present study, and also that miR-99a can suppress prostate cancer cell proliferation and prostate-specific antigen expression. Rane et al. [39] clarified that low expression levels of miR-99a are relatively radiation-insensitive and that miR-99a could be a marker of radiation sensitivity and thus a therapeutic target to improve the efficiency of radiotherapy. As previously reported, miR-99a may play important roles in cancers via target genes. For example, miR-99a might inhibit cell proliferation through

targeting TNFAIP8 in osteosarcoma cells [40]. In breast cancer, miR-99a might inhibit aggressive tumor phenotypes via regulating *HOXA1* [41]. However, miR-99a has been shown to promote cell proliferation via targeting *FGFR3* in ovarian cancer cells [42].

From the findings of the present study, it might be possible to hypothesize that miR-99a-3p has a role in prostate cancer by targeting the *PPP3CA* or *HYOU1* genes. As previously reported, *PPP3CA* is a target of miR-145 and thus be involved in caspase-dependent and caspase-independent cell death in urothelial cancer cells [43]. Also, *PPP3CA* has been shown to have a role in breast cancer, lung cancer, and Wilson’s disease [44-46]. The *HYOU1* gene has been found to be upregulated in nasopharyngeal carcinoma and may act as a molecular biomarker for the progression and prognosis of this type of cancer [47]. Also, the expression of the *HYOU1* gene is associated with lymph node involvement in colorectal cancer [48]. However, the findings of the present study are preliminary, and the roles of the *PPP3CA* and *HYOU1* genes in prostate cancer should be confirmed by both further functional and clinical studies.

Conclusions

The findings of this study showed that in patients with prostate cancer, expression of microRNA-99a-3p (miR-99a-3p) was associated with the Wnt and vascular endothelial growth factor (VEGF) signaling pathways and inhibited the expression of the protein phosphatase 3 catalytic subunit alpha (*PPP3CA*) gene and the hypoxia upregulated protein 1 (*HYOU1*) gene. The Wnt signaling pathway has been previously reported to be associated with metastasis, proliferation, apoptosis, and the cell cycle in prostate cancer [49-51]. In previously published studies, the VEGF signaling pathway has been shown to be associated with tumor angiogenesis and tumor progression [52-55]. Therefore, from the findings of this study, miR-99a-3p might have a role in prostate cancer by targeting the *PPP3CA* or *HYOU1* and contributing to the Wnt and VEGF signaling pathways. However, these preliminary findings require further molecular and functional studies and large-scale controlled clinical studies to determine the role of microRNAs, including miR-99a-3p, in prostate cancer.

Acknowledgments

The authors thank The Cancer Genome Atlas (TCGA), the Gene Expression Omnibus (GEO), and ArrayExpress for providing the data.

Conflict of interest

None.

References:

1. Cheerla N, Gevaert O: MicroRNA based pan-cancer diagnosis and treatment recommendation. *BMC Bioinformatics*, 2017; 18: 32
2. Sekhon K, Bucay N, Majid S et al: MicroRNAs and epithelial-mesenchymal transition in prostate cancer. *Oncotarget*, 2016; 7: 67597–611
3. Janiczek M, Szyberg L, Kasperska A et al: Immunotherapy as a promising treatment for prostate cancer: A systematic review. *J Immunol Res*, 2017; 2017: 4861570
4. Wadosky KM, Koochekpour S: Molecular mechanisms underlying resistance to androgen deprivation therapy in prostate cancer. *Oncotarget*, 2016; 7: 64447–70
5. Zhou P, Ma L, Zhou J et al: miR-17-92 plays an oncogenic role and conveys chemo-resistance to cisplatin in human prostate cancer cells. *Int J Urol*, 2016; 48: 1737–48
6. Liu J, Chen Z, Wang T et al: Influence of four radiotracers in PET/CT on diagnostic accuracy for prostate cancer: a bivariate random-effects meta-analysis. *Cell Physiol Biochem*, 2016; 39: 467–80
7. Storm M, Sheng X, Arnoldussen YJ, Saatcioglu F: Prostate cancer and the unfolded protein response. *Oncotarget*, 2016; 7: 54051–66
8. Park SH, Keller ET, Shiozawa Y: Bone marrow microenvironment as a regulator and therapeutic target for prostate cancer bone metastasis. *Calcif Tissue Int*, 2018; 102(2): 152–62
9. Deng G, Zheng X, Jiang P et al: Notch1 suppresses prostate cancer cell invasion via the metastasis-associated 1-KISS-1 metastasis-suppressor pathway. *Oncol Lett*, 2017; 14: 4477–82
10. Mao Y, Xu X, Wang X et al: Is angiotensin-converting enzyme inhibitors/angiotensin receptor blockers therapy protective against prostate cancer? *Oncotarget*, 2016; 7: 6765–73
11. Heinemann FM, Jindra PT, Bockmeyer CL et al: Glomerulocapillary miRNA response to HLA-class I antibody *in vitro* and *in vivo*. *Sci Reports*, 2017; 7: 14554
12. Santos PRB, Coutinho-Camillo CM, Soares FA et al: MicroRNAs expression pattern related to mast cell activation and angiogenesis in paraffin-embedded salivary gland tumors. *Pathol Res Pract*, 2017; 213(12): 1470–76
13. Gao Q, Yao X, Zheng J: MiR-323 inhibits prostate cancer vascularization through adiponectin receptor. *Cell Physiol Biochem*, 2015; 36: 1491–98
14. Zhao S, Han J, Zheng L et al: MicroRNA-203 regulates growth and metastasis of breast cancer. *Cell Physiol Biochem*, 2015; 37: 35–42
15. Chang HY, Ye SP, Pan SL et al: Overexpression of miR-194 reverses HMG2A-driven signatures in colorectal cancer. *Theranostics*, 2017; 7: 3889–900
16. Ghosh T, Varshney A, Kumar P et al: MicroRNA-874 mediated inhibition of the major G1/S phase cyclin, CCNE1 is lost in osteosarcomas. *J Biol Chem*, 2017; 292(52): 21264–81
17. Pang C, Liu M, Fang W et al: MiR-139-5p is increased in the peripheral blood of patients with prostate cancer. *Cell Physiol Biochem*, 2016; 39: 1111–17
18. Li J, Yang X, Guan H et al: Exosome-derived microRNAs contribute to prostate cancer chemoresistance. *Int J Oncol*, 2016; 49: 838–46
19. Sun D, Lee YS, Malhotra A et al: miR-99 family of microRNAs suppresses the expression of prostate-specific antigen and prostate cancer cell proliferation. *Cancer Res*, 2011; 71: 1313–24
20. Shen S, Lin Y, Yuan X et al: Biomarker microRNAs for diagnosis, prognosis and treatment of hepatocellular carcinoma: A functional survey and comparison. *Sci Rep*, 2016; 6: 38311
21. Ji W, Sun B, Su C: Targeting microRNAs in cancer gene therapy. *Genes (Basel)*, 2017; 8(1): pii: E21
22. Molina-Pinelo S, Carnero A, Rivera F et al: MiR-107 and miR-99a-3p predict chemotherapy response in patients with advanced colorectal cancer. *BMC Cancer*, 2014; 14: 656
23. Xiong H, Li Q, Liu S et al: Integrated microRNA and mRNA transcriptome sequencing reveals the potential roles of miRNAs in stage I endometrioid endometrial carcinoma. *PLoS One*, 2014; 9: e110163
24. Li D, Liu X, Lin L et al: MicroRNA-99a inhibits hepatocellular carcinoma growth and correlates with prognosis of patients with hepatocellular carcinoma. *J Biol Chem*, 2011; 286: 36677–85
25. Bornstein S, Schmidt M, Choonoo G et al: IL-10 and integrin signaling pathways are associated with head and neck cancer progression. *BMC Genomics*, 2016; 17: 38
26. Li Y, Kang K, Krahn JM et al: A comprehensive genomic pan-cancer classification using The Cancer Genome Atlas gene expression data. *BMC Genomics*, 2017; 18: 508
27. Zeng JH, Xiong DD, Pang YY et al: Identification of molecular targets for esophageal carcinoma diagnosis using miRNA-seq and RNA-seq data from The Cancer Genome Atlas: A study of 187 cases. *Oncotarget*, 2017; 8: 35681–99
28. Ferreira MJ, Pires-Luis AS, Vieira-Coimbra M et al: SETDB2 and RIOX2 are differentially expressed among renal cell tumor subtypes, associating with prognosis and metastization. *Epigenetics*, 2017; 12(12):1057–64
29. Zeng Y, Wang T, Liu Y et al: LncRNA PVT1 as an effective biomarker for cancer diagnosis and detection based on transcriptome data and meta-analysis. *Oncotarget*, 2017; 8: 75455–66
30. Mou T, Zhu D, Wei X et al: Identification and interaction analysis of key genes and microRNAs in hepatocellular carcinoma by bioinformatics analysis. *World J Surg Oncol*, 2017; 15: 63
31. Ge QM, Huang CM, Zhu XY et al: Differentially expressed miRNAs in sepsis-induced acute kidney injury target oxidative stress and mitochondrial dysfunction pathways. *PLoS One*, 2017; 12: e0173292
32. Wang X, Li Y, Xu G et al: Mechanism study of peptide GMBP1 and its receptor GRP78 in modulating gastric cancer MDR by iTRAQ-based proteomic analysis. *BMC Cancer*, 2015; 15: 358
33. Liu D, Liu P, Cao L et al: Screening the key genes of hepatocellular adenoma via microarray analysis of DNA expression and methylation profiles. *Oncol Lett*, 2017; 14: 3975–80
34. Liao J, Wei B, Chen H et al: Bioinformatics investigation of therapeutic mechanisms of Xuesaitong capsule treating ischemic cerebrovascular rat model with comparative transcriptome analysis. *Am J Transl Res*, 2016; 8: 2438–49
35. Zhang Y, He RQ, Dang YW et al: Comprehensive analysis of the long non-coding RNA HOXA11-AS gene interaction regulatory network in NSCLC cells. *Cancer Cell Int*, 2016; 16: 89
36. Franceschini A, Szklarczyk D, Frankild S et al: STRING v9.1: Protein-protein interaction networks, with increased coverage and integration. *Nucleic Acids Res*, 2013; 41: D808–15
37. Dai Y, Jiang JB, Wang YL et al: Functional and protein-protein interaction network analysis of colorectal cancer induced by ulcerative colitis. *Mol Med Rep*, 2015; 12: 4947–58
38. Friard O, Re A, Taverna D et al: CircuitsDB: a database of mixed microRNA/transcription factor feed-forward regulatory circuits in human and mouse. *BMC Bioinformatics*, 2010; 11: 435
39. Rane JK, Erb HH, Nappo G et al: Inhibition of the glucocorticoid receptor results in an enhanced miR-99a/100-mediated radiation response in stem-like cells from human prostate cancers. *Oncotarget*, 2016; 7: 51965–80
40. Xing B, Ren C: Tumor-suppressive miR-99a inhibits cell proliferation via targeting of TNFAIP8 in osteosarcoma cells. *Am J Transl Res*, 2016; 8: 1082–90
41. Wang X, Li Y, Qi W et al: MicroRNA-99a inhibits tumor aggressive phenotypes through regulating HOXA1 in breast cancer cells. *Oncotarget*, 2015; 6: 32737–47
42. Jiang H, Qu L, Wang Y et al: miR-99a promotes proliferation targeting FGFR3 in human epithelial ovarian cancer cells. *Biomed Pharmacother*, 2014; 68: 163–69
43. Ostendorf MS, Bramsen JB, Lamy P et al: miR-145 induces caspase-dependent and -independent cell death in urothelial cancer cell lines with targeting of an expression signature present in Ta bladder tumors. *Oncogene*, 2010; 29: 1073–84
44. Gabrovská PN, Smith RA, Haupt LM, Griffiths LR: Investigation of two Wnt signalling pathway single nucleotide polymorphisms in a breast cancer-affected Australian population. *Twin Res Hum Genet*, 2011; 14: 562–67
45. Lee BH, Kim JH, Kim JM et al: The early molecular processes underlying the neurological manifestations of an animal model of Wilson's disease. *Metallomics*, 2013; 5: 532–40
46. Campbell JD, Alexandrov A, Kim J et al: Distinct patterns of somatic genome alterations in lung adenocarcinomas and squamous cell carcinomas. *Nat Genet*, 2016; 48: 607–16
47. Zhou Y, Liao Q, Li X et al: HYOU1, regulated by LPLUNC1, is up-regulated in nasopharyngeal carcinoma and associated with poor prognosis. *J Cancer*, 2016; 7: 367–76

48. Slaby O, Sobkova K, Svoboda M et al: Significant overexpression of Hsp110 gene during colorectal cancer progression. *Oncol Rep*, 2009; 21: 1235–41
49. Wang L, Dehm SM, Hillman DW et al. A prospective genome-wide study of prostate cancer metastases reveals association of Wnt pathway activation and increased cell cycle proliferation with primary resistance to abiraterone acetate-prednisone. *Ann Oncol*, 2018; 29(2): 352–60
50. Shin S, Im HJ, Kwon YJ et al: Human steroid sulfatase induces Wnt/beta-catenin signaling and epithelial-mesenchymal transition by upregulating Twist1 and HIF-1alpha in human prostate and cervical cancer cells. *Oncotarget*, 2017; 8: 61604–17
51. Zheng Y, Trivedi T, Lin RC et al: Loss of the vitamin D receptor in human breast and prostate cancers strongly induces cell apoptosis through down-regulation of Wnt/beta-catenin signaling. *Bone Res*, 2017; 5: 17023
52. Liu L, Liang Z, Guo K, Wang H: Relationship between the expression of CD133, HIF-1alpha, VEGF and the proliferation and apoptosis in hypoxic human prostate cancer cells. *Oncol Lett*, 2017; 14: 4065–68
53. Zhang W, Shou WD, Xu YJ et al: Low-frequency ultrasound-induced VEGF suppression and synergy with dendritic cell-mediated anti-tumor immunity in murine prostate cancer cells *in vitro*. *Sci Rep*, 2017; 7: 5778
54. Alshaker H, Wang Q, Bohler T et al: Combination of RAD001 (everolimus) and docetaxel reduces prostate and breast cancer cell VEGF production and tumour vascularisation independently of sphingosine-kinase-1. *Sci Rep*, 2017; 7: 3493
55. Terzuoli E, Donnini S, Finetti F et al: Linking microsomal prostaglandin E Synthase-1/PGE-2 pathway with miR-15a and -186 expression: Novel mechanism of VEGF modulation in prostate cancer. *Oncotarget*, 2016; 7: 44350–64